journal

J. Am. Ceram. Soc., 94 [3] 932–937 (2011)
DOI: 10.1111/j.1551-2916.2010.04167.x

Formation of Cotunnite Phase in ZrO_2 under Uniaxial Stress: A First Principles Study

Hülya Öztürk[‡] and Murat Durandurdu[†,‡,§]

[‡]Fizik Bölümü, Ahi Evran Üniversitesi, Kırşehir 40100, Turkey

[§]Department of Physics, University of Texas at El Paso, El Paso, Texas 79968

Using a constant pressure *ab initio* technique, we study the response of ZrO_2 to uniaxial stresses and find two different phase transformations; the application of uniaxial stress along the [010] and [100] directions yields a direct phase transformation from the baddeleyite structure to the $P2_1/m$ and *Pnma* structures, respectively. Conversely, we observe structural failure of ZrO_2 when it is compressed along the [001] axis.

I. Introduction

Zirconia (ZrO_2), an important ceramic, possesses very interesting physical properties such as high melting temperature, high refractive index, low thermal conductivity, hardness, and corrosion barrier properties. It has a wide range of applications such as durable thermal barrier coatings and optical coatings absorbing harmful ultraviolet radiation, as well as an important component in oxygen sensors, catalytic converters or in chemically passivating surfaces.

Pure zirconia in the equilibrium state exists in three polymorphic forms: the monoclinic baddeleyite structure ($P2_1/c$) with cations located in sevenfold coordination environments below 1170°C, the tetragonal phase (space group $P4_2/nmc$) with distorted eightfold coordination in the temperature range 1170°–2370°C, and finally the cubic structure (space group $Fm3m$) having perfect eightfold coordination of cations above 2370°C. The tetragonal and cubic phases of zirconia could be stabilized by doping them with other oxides such as MgO and Y_2O_3. Depending on the dopant concentration, ZrO_2 remains cubic or tetragonal even at room temperature.

The high-pressure behavior of ZrO_2 has been the subject of many experimental and theoretical investigations. Yet, there are still unknowns and controversies about its high-pressure phases.[1–13] The monoclinic baddeleyite structured ($P2_1/c$) ZrO_2 at ambient conditions exhibits rich polymorphism at high pressures and temperatures. In two experimental studies,[1,2] a pressure-induced phase transformation from the baddeleyite structure ($P2_1/c$) to an orthorhombic phase with space group *Pbcm* around 4 GPa was reported but this transformation was not confirmed in later studies[3–6] and instead a phase transition into an orthorhombic state with space group *Pbca* was demonstrated in those experiments. Several experiments proposed the formation of another orthorhombic phase with space group *Pnma,* isostructural to the ninefold coordinated cotunnite ($PbCl_2$) structure[7–9] at high pressure. On the other hand, Léger *et al.*[4] obtained the baddeleyite→orthorhombic-I (*Pbca*)→orthorhombic-II→orthorhombic-III phase transformation at room temperature around 10, 25, and 42 GPa, respectively. The symmetry of orthorhombic-II and orthorhombic-III has not been identified yet to our knowledge. Arashi *et al.*[10] observed a phase transition at 13 GPa, but were not able to verify a cotunnite structure. Additionally, the authors found a quenchable tetragonal phase about 35 GPa (most likely space groups were $P4/m$, $P4_2/n$, $P4/mmm$, or $P4/mbm$). In addition to these structures, the tetragonal (MnF_2) and hexagonal phases[9,11] were observed in experiments as well. Very recent high-pressure experiment[14] clearly demonstrated the existence of the cotunnite phase in ZrO_2, eliminating some doubts about the phase diagram of in ZrO_2. Therefore, the transition sequence in ZrO_2 is expected to be $P2_1/c \rightarrow Pbca \rightarrow Pnma$.

In order to better understand the pressure-induced phase transition in ZrO_2 and to explain the controversies observed experiments, we studied its behaviors under pure hydrostatic pressure using a constant pressure *ab initio* technique[15] and found two first-order phase transformations in ZrO_2: the baddeleyite structure first transformed into an orthorhombic structure (*Pbcm*) and then a tetragonal structure ($P4/nmm$). Regrettably, our finding does not agree with the $P2_1/c \rightarrow Pbca \rightarrow Pnma$ transformation mechanism. The origin of the disagreement is not clear but we suspect that it is related to kinetic. Our simulations were performed at 0 K (relaxation of structure under pressure) while experiments were performed at room or high temperatures. Consequently at low temperatures, ZrO_2 might follow the $P2_1/c \rightarrow Pbcm \rightarrow P4/nmm$ transformations as predicted in the simulations. Certainly, further experimental and theoretical studies are need to clarify this issue.

In addition to hydrostatic pressure, studies of the structural and mechanical responses of materials at finite strain are crucial for our understanding of many areas such as phase transformation, theoretical strength, crack propagation, nanotechnology, and the investigation of epitaxial thin film. However, the determination of stable crystalline structures under stresses has been the subject of a long theoretical debate.[16–20] Wang *et al.*[19] pointed out the existence of a Gibbs free energy for systems under hydrostatic pressure but a true thermodynamic potential does not exist under anisotropic stress. In the past, nonhydrostatic conditions have been investigated for different reasons.[20–26]

In this work, we explore the response of ZrO_2 to uniaxial stresses to better understand its phase transformations. We find an orthorhombic structure with space group *Pnma* (cotunnite) and a monoclinic crystal having space group $P2_1/m$ with the application of uniaxial stress along [100] and [010] directions, respectively while we observe structural failure when it is compressed along the [001] direction. Our findings provide new perspectives on high-pressure phases of ZrO_2.

II. Computational Method

The calculations were carried out using the SIESTA code.[27] The method is based on the density functional theory adopting a localized linear combination of atomic orbital basis sets for the description of valence electrons and norm-conserving nonlocal

L-Q. Chen—contributing editor

Manuscript No. 27249. Received December 14, 2009; approved September 10, 2010.
[†]Author to whom correspondence should be addressed. e-mail: mdurandurdu@utep.edu

pseudopotentials for atomic core. The pseudopotentials were constructed using Troullier and Martins scheme.[28] The exchange correlation energy was calculated using the generalized gradient approximation of Perdew, Burke, and Ernzerhof.[29] The double-σ plus polarized orbitals were used. A real space grid was equivalent to a plane wave cut-off energy of 150 Ry. The simulation cell with two unit cells of x, y, and z directions consists of 96 atoms with periodic boundary conditions. We used γ-point sampling for the Brillouin zone integration for the supercell simulations. The system was first relaxed at zero stress, and then its response to uniaxial compressive stresses is examined in three different directions: [100], [010], and [001]. For each case of uniaxial compressions, the stress is applied along one direction while the other stress components are initially set to zero. For each value of the applied stress, the structure was allowed to relax and find its equilibrium volume and the corresponding energy by optimizing its lattice vectors and atomic positions together until the stress tolerance was <0.5 GPa and the maximum atomic force was smaller than 0.01 eV/Å. For minimization of geometries, a variable-cell shape conjugate-gradient method under a constant stress was used. To ensure that the stress path was continuous, the starting position at each stress step was taken from the relaxed coordinates of previous steps.

We applied the variable-cell shape conjugate-gradient method to study pressure-induced phase transformations in various materials and found that it is very successful in reproducing experimentally observed high-pressure phases. However, the predicted transition pressures in our simulations are considerably larger than the experimentally observed transition pressures because simulated systems have to cross a significant energy barrier to transform from one phase to another.[30] This trend is appropriate to the particular conditions of the simulations. The use of periodic boundary conditions in the simulations eliminates surfaces and leads to an additional coupling of the ions in the simulation box. The lack of any defects in the simulated structure also suppresses nucleation and growing, in a contrast to experiments. These tend to favor a phase change, in which the whole system undergoes the phase transformation as a collective movement of all atoms. As a result, systems cross a significant energy barrier to transform from one phase to another one. Additionally, the absence of thermal motion (relaxation of the structure at constant pressure) in our simulations shifts the transitions to a higher pressure. On the other hand, the thermodynamic theorem does not take into account the possible existence of such an activation barrier separating the two structural phases and the thermal motion and hence usually yield reasonable transition pressures relative to experiments. Therefore, as a next step, we use the thermodynamic criterion of equal free energies to predict accurate critical stresses for the phase transitions obtained using the variable-cell shape conjugate-gradient method under uniaxial stresses.

The relative stability of different phases under hydrostatic pressure can be determined by a simple comparison of their static enthalpy

$$H_{\text{hydrostatic}} = E_{\text{tot}} + PV \tag{1}$$

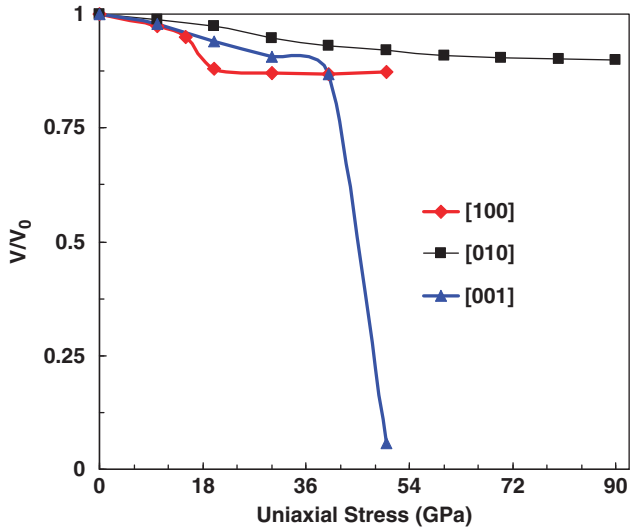

Fig. 1. The volume change as a function of uniaxial stress.

where E_{tot} is the energy, V is the volume, and P is the external pressure. In order to calculate the enthalpy of ZrO_2 phases, we first studied their total energy as a function of volume and then fitted the energy–volume data to the third-order Birch–Murnaghan equation of state. From the energy–volume curves, we obtained the pressure ($P = -\mathrm{d}E_{\text{tot}}/\mathrm{d}V$) and the hydrostatic enthalpy of the phases.

For the case of uniaxial compression, the enthalpy is

$$H_{\text{uniaxial}} = E_{\text{tot}} + A_{ij}\sigma_k x_k \tag{2}$$

where E_{tot} is the energy, σ_k is the applied stress along the k-direction, x_k is the lattice parameter in the k-direction, A_{ij} is the cross-section area of the unit cell perpendicular to the stress direction (note that ZrO_2 has a monoclinic structure at ambient conditions and hence β-angle should be taken account for A_{ij} calculations), and $A_{ij}\sigma_k x_k$ is the external work (see Sarasamak *et al.*[31] for more information). In order to calculate enthalpy under uniaxial stresses, we studied the baddeleyite, $P2_1/m$, and *Pnma* phases under uniaxial stresses using the variable cell simulation technique. After the structures were relaxed at different uniaxial stresses, E_{tot} and the lattice vectors, $\boldsymbol{a}$, $\boldsymbol{b}$, $\boldsymbol{c}$ (hence A_{ij}) were determined in the output file. Again, to guarantee that the stress path was continuous, the starting position at each stress step was taken from the relaxed coordinates of previous steps.

For the enthalpy calculations, we considered the unit cell for ZrO_2 phases in order to reduce computational efforts. The Brillouin zone integration was performed with automatically generated $6 \times 6 \times 6$ k-point mesh for the phases following the convention of Monkhorst and Pack.[32]

In order to determine the symmetry of the phases formed under uniaxial compressions in the simulations, we used the KPLOT program[33] that provides detailed information about

Table I. The atomic fractional coordinates and the equilibrium lattice parameters of the $P2_1/m$ and *Pnma* phases

Structure	a (Å)	b (Å)	c (Å)	x	y	z
$P2_1/c$	5.1676	5.2445	5.3342	Zr: 0.224711	0.04478	0.790665
				O: 0.430636	0.334425	0.656823
				O: 0.050048	0.759832	0.520276
$P2_1/m$	5.4771	3.4895	3.8968	Zr: 0.269913	0.25	0.16598
				O: 0.434687	0.25	0.73484
				O: 0.918064	0.25	0.76926
Pnma	5.6476	3.1358	6.7218	Zr: 0.254596	0.25	0.61834
				O: 0.14295	0.25	0.92571
				O: 0.01687	0.25	0.33826

The monoclinic β angle is 104.2591° for $P2_1/m$. In order to compare $P2_1/m$ with $P2_1/c$ phase, the coordinates and lattice parameters of the $P2_1/c$ phase is also presented in the table.

space group, cell parameters, and atomic position of a given structure. For the symmetry analysis, we used 0.2 Å, 4°, and 0.7 Å tolerances for bond lengths, bond angles, and interplanar spacing, respectively.

III. Results

(1) Constant Stress Calculations

Figure 1 shows the variation of volume as a function of uniaxial stresses. As seen from the figure, the phase transition under uniaxial compression along [100] axis is accompanied by a volume change and it is a first order nature. The volume change is about 10%. The structural analysis using the KPLOT program reveals a phase transformation into the cotunnite phase at 20 GPa (see Fig. 2). The lattice parameters of and the atomic position of this phase at 20 GPa are given in Table I. In this phase, Zr atoms are ninefold coordinated and hence owing to this phase transformation, each Zr atom forms two new bonds. The new bonds form between Zr atoms and O atoms at distances of 3.88 and 4.47 Å in the baddeliyette structure, demonstrating that the transformation is associated with the significant decrease of the second neighbor distances. The bond lengths in the cotunnite phase are not uniform and range from 2.21 to 2.503 Å. The formation of the cotunnite phase under hydrostatic pressure via the *Pbca* phase has been observed in several experiments.[7–9] Here, we also predict that the formation of the cotunnite phase under uniaxial compression along the [100] direction is achievable as well.

The symmetry analysis indicates a phase change at 30 GPa for the application of uniaxial stress along [010] direction, which is also first-order nature. The volume change is about 3%. This phase has still monoclinic structure with the monoclinic angle of 104.2° but its symmetry is $P2_1/m$ (see Fig. 2). Its lattice constants and atomic positions are presented in Table I. In this structure, the coordination number does not change with respect to that in the baddeleyite phase. The Zr–O separations are in the range of 2.05–2.36 Å. This phase is stable up to 90 GPa, the maximum stress studied. As can be seen from Table I, the internal positions of the $P2_1/m$ phase, in particular, the y component are different from those of baddeleyite phase.

The uniaxial loading along the [001] direction yields structural failure, which is identified from the formation of two-dimensional layered structure with a dramatic volume drop

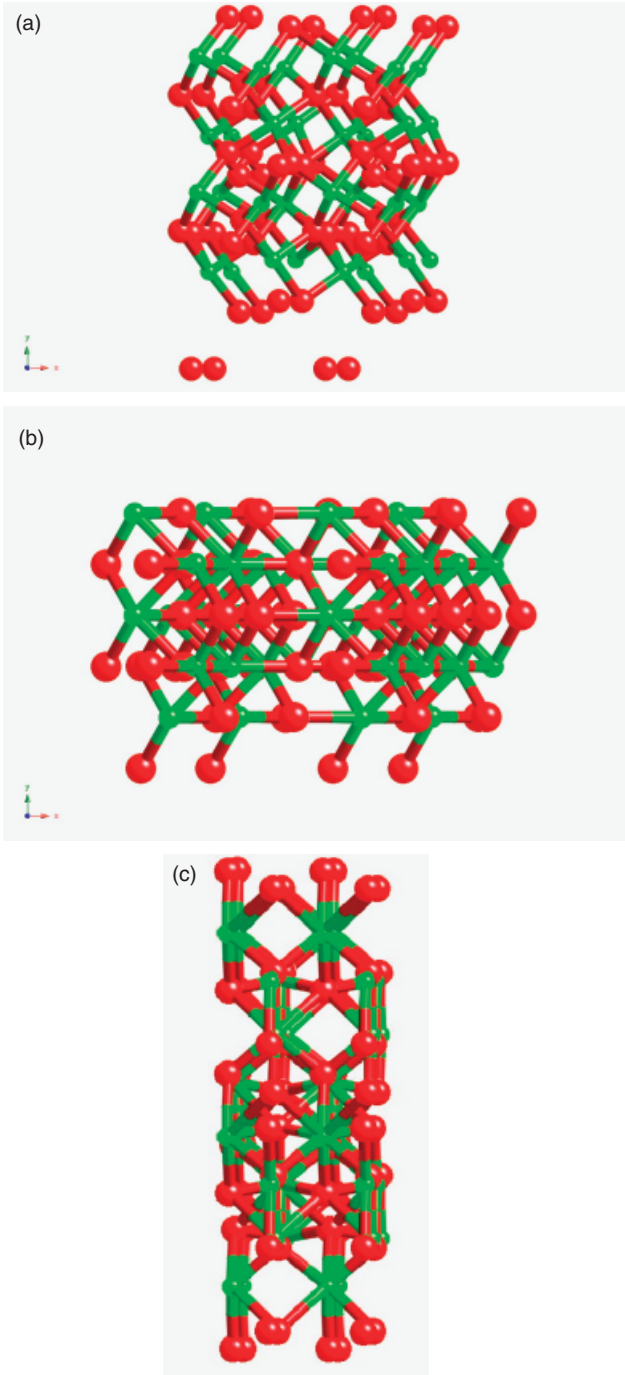

Fig. 2. (Color online) Crystal structures of ZrO_2: baddeleyite (a) at zero-pressure, $P2_1/m$ (b) at 30 Gpa, and *Pnma* (c) at 20 GPa.

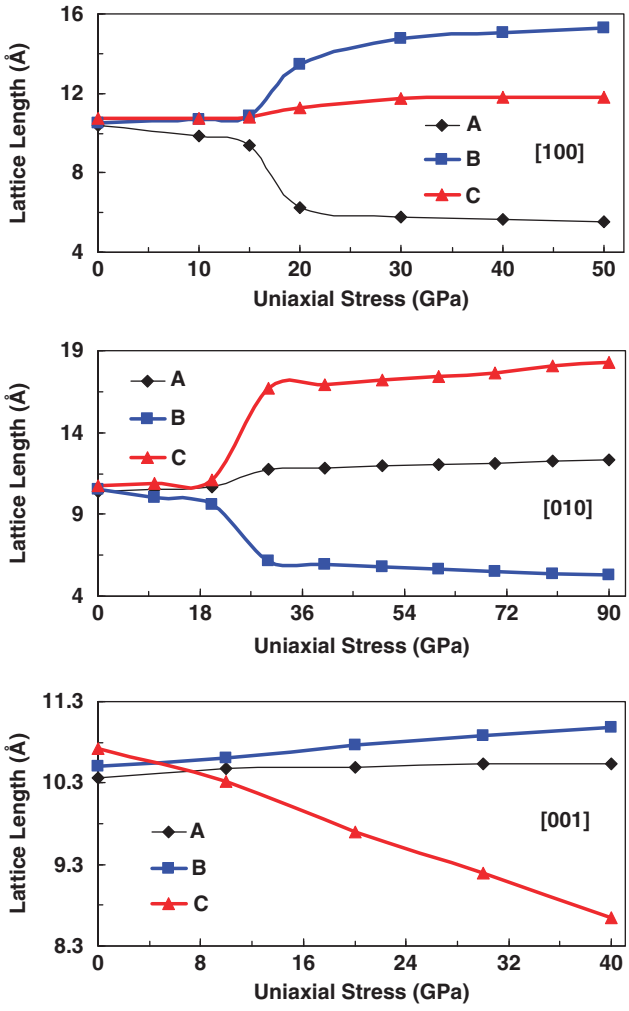

Fig. 3. (Color online) Change in the simulation cell lengths (The simulation cell with two unit cells of x, y, and z directions consists of 96 atoms). The simulation cell vectors **A**, **B**, and **C** are initially along the [100], [010], and [001]directions, respectively. The magnitude of these vectors is plotted in the figure.

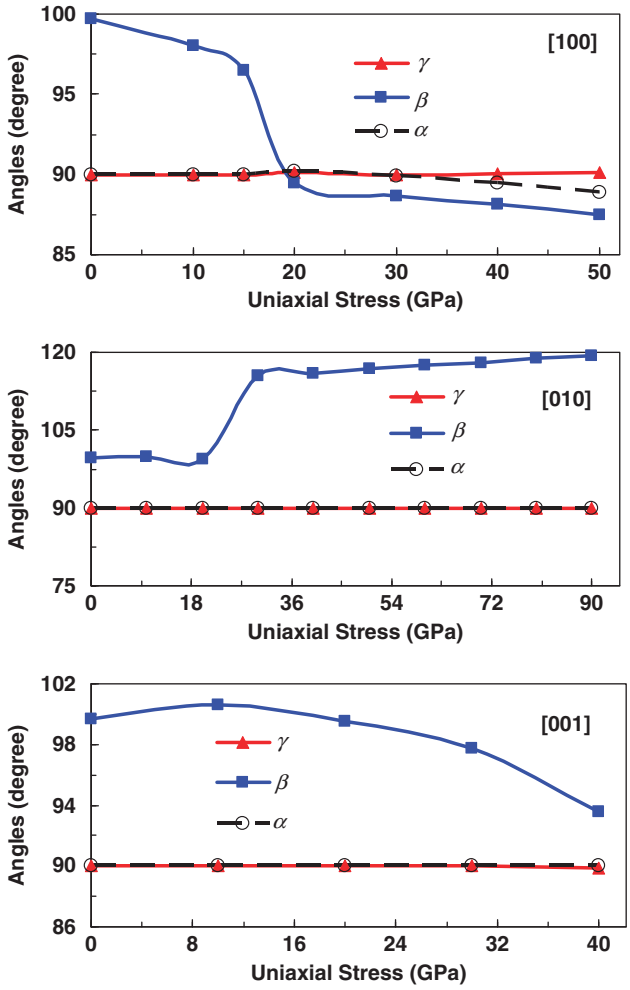

Fig. 4. The variation of simulation cell angles. The β is the angle between **A** and **C** vectors.

at 50 GPa. During the failure, the structure is dramatically expanded along [100] and [010] directions and some bonds are broken.

The simulation cell lengths and angles as a function of the applied uniaxial stresses are depicted in Figs. 3 and 4 and they can provide substantial information about the phase transformation at the atomistic level. For all cases considered in this study, the ZrO_2 is compressed along the applied stress direction while it is expanded along the other directions but the expansion relative to compression is small and hence the volume decreases under uniaxial stresses. As seen from the Fig. 4, during the uniaxial loadings, the monoclinic angle changes gradually, indicating that the structure undergoes shear deformations. In the case of the [100] direction loading, the monoclinic angle becomes about 90° owing to the phase transformation as seen in the hydrostatic compression.[15] On the other hand, the monoclinic angle increases to about 116° for the case of [010] uniaxial compression. Consequently, in both phase transformations, the shear deformation plays an important role but it cannot be the main mechanism alone because ZrO_2 under pure hydrostatic compression also undergoes a shear deformation (the monoclinic angle becomes 90°) and transforms into the orthorhombic structure (*Pbcm*).[15] Therefore, these phase transformations are due to the coupling of shear deformations and the change of lattice parameters.

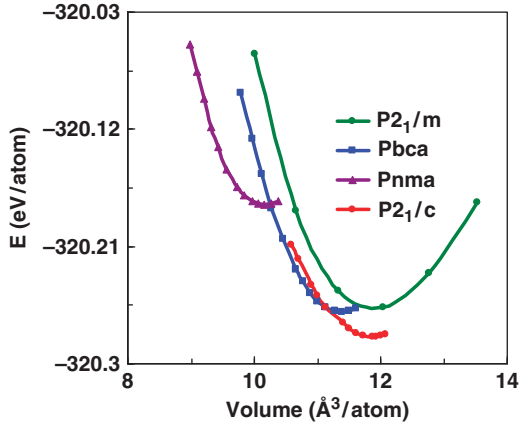

Fig. 5. (Color online) The computed energy of ZrO_2 phases as a function of volume.

(2) *Energy–Volume and Enthalpy Calculations*

In order to compare energetic of the phases formed under uniaxial stresses with the other forms of ZrO_2, we calculate their energy–volume relations and plot some of them in Fig. 5 (see Öztürk and Durandurdu[15] for more details). Comparing the baddeleyite and $P2_1/m$ phases, we observe that the volume per atom of the $P2_1/m$ phase is slightly larger (about 1.4%) than that of the baddeleyite phase. The energy difference between the two phases is 22.3 meV/atom. This value is comparable with the energy difference between baddeleyite and its high-pressure phase *Pbca* (19 meV/atom), indicating that the energetics of the $P2_1/m$ is also favorable. However, when the common tangent lines are considered between the energy–volume curve of

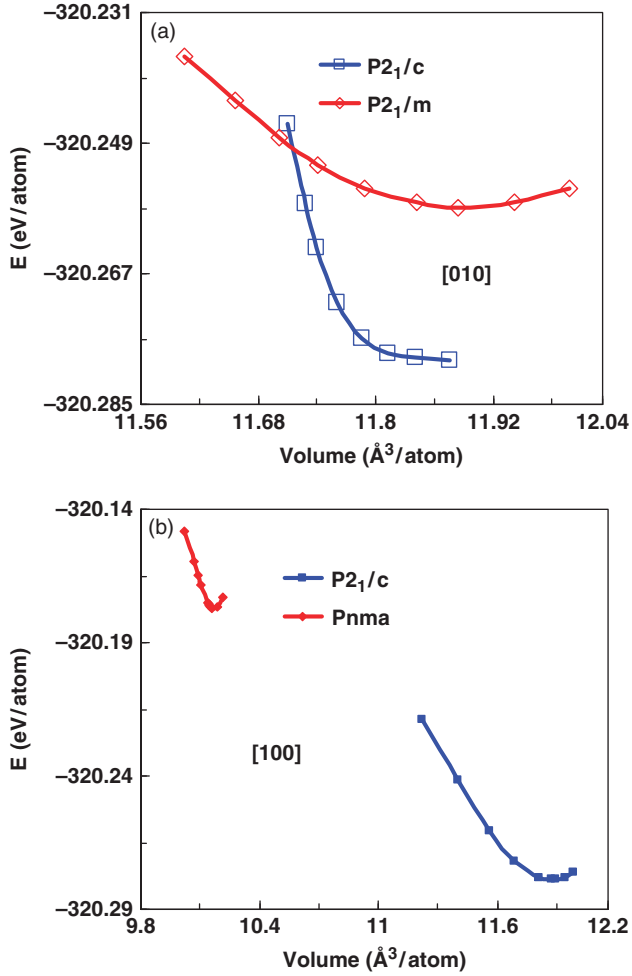

Fig. 6. (a) The energy curve of the baddeleyite and $P2_1/m$ phases under uniaxial compression along the [010] direction. (b) The energy curve of the baddeleyite and *Pnma* phases under uniaxial compression along the [100] direction.

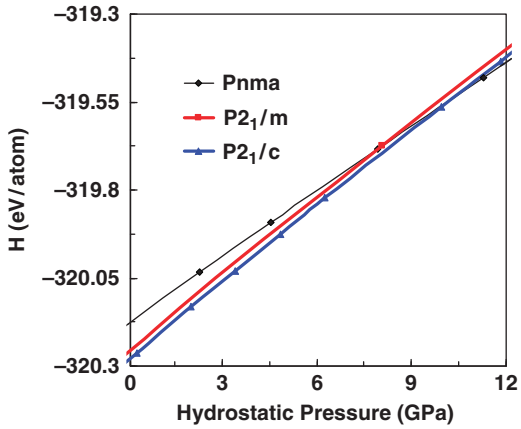

Fig. 7. The calculated enthalpy curve of the baddeleyite, $P2_1/m$, and *Pnma* phases under hydrostatic pressure.

the baddeleyite phase and that of the $P2_1/m$ phase, a pressure-induced phase transformation between these two phases under hydrostatic pressure is impossible and hence the $P2_1/m$ phase has not been observed experimentally so far. On the other hand, as can clearly be seen from Fig. 6, the energy curve of the baddeleyite and $P2_1/m$ phases under uniaxial stress along the [010] direction crosses around 11.72 $Å^3$/atom. Therefore, one expects to see a possible phase transformation between these phases. In order to predict accurate critical stresses for the phase transformations observed in the present study, we calculate the enthalpy of the phases using the Eqs. 1 and 2. The enthalpies are plotted as a function of hydrostatic pressure in Fig. 7 and of uniaxial stresses in Fig. 8. Accordingly, the hydrostatic enthalpy curves of the baddeliyette and $P2_1/m$ are parallel to each other and they do not cross, meaning that the baddeliyette and $P2_1/m$ phase transition is thermodynamically impossible under hydrostatic pressure, whereas the uniaxial enthalpy curve of the baddeliyette phase crosses with that of the $P2_1/m$ crystal around 8.3 GPa. The baddeliyette to cotunnite phase transition under uniaxial stress is predicted to occur near 10.0 GPa. Therefore, we expect that these phase transformations occur around 8–10 GPa in experiments.

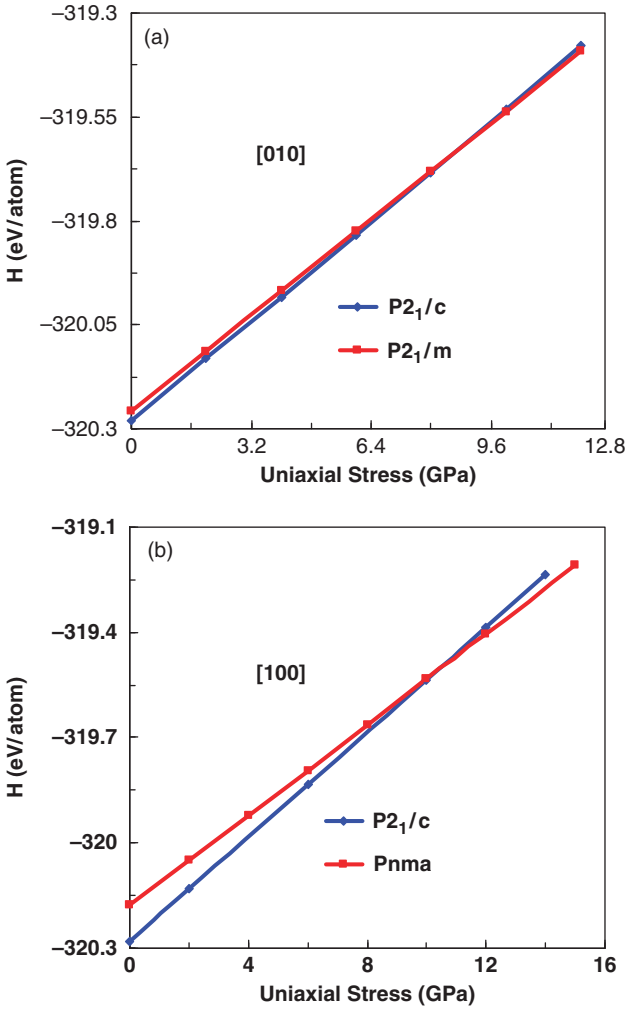

Fig. 8. The enthalpy curve of (a) the baddeleyite and $P2_1/m$ phases under uniaxial stress along the [010] axis, (b) the baddeleyite and *Pnma* phases under uniaxial stress along the [010] axis.

IV. Conclusions

We have used a constant pressure *ab initio* technique to study the behavior of ZrO_2 under uniaxial stresses and predicted two structural phase transformations. The uniaxial compression along [100] produces a direct phase change to a ninefold coordinated cotunnite phase. This phase transformation is due to the decrease of the second neighbor distances. The uniaxial loading along [010] axis results in a monoclinic state having $P2_1/m$ symmetry. This phase is stable up to 90 GPa. On the other hand, we observe structural failure of ZrO_2 when it is compressed along the [001] axis. The cotunnite phase is suggested as a candidate for a useful superhard material. Therefore, its formation is particularly important. The $P2_1/m$ phase might also offer new applications in technology.

Acknowledgments

The visit of M. D. to Ahi Evran Üniversitesi was facilitated by the Scientific and Technical Research Council of Turkey (TÜBİTAK) BIDEB-2221.

References

[1]Y. Kudoh, H. Takeda, and H. Arashi, "In Situ Determination of Crystal Structure for High Pressure Phase of ZrO_2 Using a Diamond Anvil and Single Crystal X-Ray Diffraction Method," *Phys. Chem. Miner.*, **13**, 233–7 (1986).
[2]A. H. Heuer, V. Lanteri, S. C. Farmer, R. Chaim, R. R. Lee, B. W. Kibbel, and R. M. Dickerson, "On the Orthorhombic Phase in ZrO_2-Based Alloys," *J. Mater. Sci.*, **24**, 124–32 (1989).
[3]O. Ohtaka, T. Yamanaka, S. Kume, N. Hara, H. Asano, and F. Izumi, "Structural Analysis o f Orthorhombic ZrO_2 by High Resolution Neutron Powder Diffraction," *Proc. Jpn. Acad. Ser. B: Phys. Biol. Sci.*, **66**, 193–6 (1990).
[4]J. M. Léger, P. E. Tomaszewski, A. Atouf, and A. S. Pereira, "Pressure-Induced Structural Phase Transitions in Zirconia under High Pressure," *Phys. Rev. B*, **47**, 14075–83 (1993).
[5]S. Desgreniers and K. Lagarec, "High-Density ZrO_2 and HfO_2: Crystalline Structures and Equations of State," *Phys. Rev. B*, **59**, 8467–72 (1999).
[6]J. Haines, J. M. Léger, S. Hull, J. P. Petitet, A. S. Pereira, C. A. Perottoni, and J. A. H. da Jornada, "Characterization of the Cotunnite-Type Phases of Zirconia and Hafnia by Neutron Diffraction and Raman Spectroscopy," *J. Am. Ceram. Soc.*, **80**, 1910–4 (1997).
[7]S. Block, J. A. H. Jornada, and G. J. Piermarini, "Pressure-Temperature Phase Diagram of Zirconia," *J. Am. Ceram. Soc.*, **68**, 497–9 (1985).
[8]J. Haines, J. M. Léger, and A. Atouf, "Crystal Structure and Equation of State of Cotunnite-Type Zirconia," *J. Am. Ceram. Soc.*, **78**, 445–8 (1995).
[9]L. C. Ming and M. H. Manghnani, pp. 135–40 *Solid State Physics Under Pressure: Recent Advances with Anvil Devices*, Edited by S. Minomura. KTK Science, Tokyo, 1985.
[10]H. Arashi, T. Yagi, S. Akimoto, and Y. Kudoh, "New High-Pressure Phase of ZrO_2 above 35 GPa," *Phys. Rev. B*, **41**, 4309–13 (1990).
[11]O. Ohtaka, T. Yamanaka, and T. Yagi, "New High-Pressure and -Temperature Phase of ZrO_2 above 1000°C at 20 GPa," *Phys. Rev. B*, **49**, 9295–8 (1994).
[12]J. E. Lowther, J. K. Dewhurst, J. M. Leger, and J. Haines, "Relative Stability of ZrO_2 and HfO_2 Structural Phases," *Phys. Rev. B*, **60**, 14485–8 (1999).
[13]J. E. Jaffe, R. A. Bachorz, and M. Gutowski, "Low-Temperature Polymorphs of ZrO_2 and HfO_2: A Density-Functional Theory Study," *Phys. Rev. B*, **72**, 144107–15 (2005).
[14]O. Ohtaka, D. Andrault, P. Bouvier, E. Schultz, and M. Mezouar, "Phase Relations and Equation of State of ZrO_2 to 100 GPa," *J. Appl. Cryst.*, **38**, 727 (2005).
[15]H. Öztürk and M. Durandurdu, "High-Pressure Phases of ZrO_2 an *Ab Initio* Constant Pressure Study," *Phys. Rev. B*, **79**, 134111 (2009).
[16]V. Sin'ko and N. A. Smirnov, "On the Elasticity under Pressure," *J. Phys.: Condens. Matter*, **16**, 8101 (2004).
[17]Z. Zhou and B. Joós, "Stability Criteria for Homogeneously Stressed Materials and the Calculation of Elastic Constants," *Phys. Rev. B*, **54**, 3841 (1996).

[18]J. Wang, S. Yip, S. R. Phillpot, and D. Wolf, "Crystal Instabilities at Finite Strain," *Phys. Rev. Lett.*, **71**, 4182 (1993).
[19]J. Wang, J. Li, S. Yip, S. Phillpot, and D. Wolf, "Mechanical Instabilities of Homogeneous Crystals," *Phys. Rev. B*, **52**, 12627 (1995).
[20]S. Subramanian and S. Yip, "Structural Instability of Uniaxially Compressed α-Quartz," *Comp. Mater. Sci.*, **23**, 116 (2002).
[21]C. Cheng, W. H. Huang, and H. J. Li, "Thermodynamics of Uniaxial Phase Transition: *Ab Initio* Study of the Diamond-to-β-Tin Transition in Si and Ge," *Phys. Rev. B*, **63**, R153202 (2001).
[22]I.-H. Lee, J.-W. Jeong, and K. J. Chang, "Invariant-Molecular-Dynamics Study of the Diamond-to-β-Sn Transition in Si under Hydrostatic and Uniaxial Compressions," *Phys. Rev. B*, **55**, 5689 (1997).
[23]H. Libotte and J. P. Gaspard, "Pressure-Induced Distortion of the β-Sn Phase in Silicon: Effects of Nonhydrostaticity," *Phys. Rev. B*, **62**, 7110–5 (2000).
[24]M. Durandurdu, "Structural Phase Transition of Ge Under Uniaxial Stress: An *Ab Initio* Study," *Phys. Rev. B*, **71**, 054112 (2005).
[25]M. Durandurdu, "Structural Phase Transformation in Gold Under Uniaxial, Tensile and Triaxial Stresses: An *Ab Initio* Study," *Phys. Rev. B*, **76**, 024102 (2007).
[26]M. Durandurdu, "Formation of an Anatase-Like Phase in Silica," *Phys. Rev. B*, **80**, 024102 (2009).
[27]P. Ordejón, E. Artacho, and J. M. Soler, "Self-Consistent Order-*N* Density-Functional Calculations for Very Large Systems," *Phys. Rev. B*, **53**, R10441–4 (1996).
[28]N. Troullier and J. M. Martins, "Efficient Pseudopotentials for Plane-Wave Calculations," *Phys. Rev. B*, **43**, 1993–2006 (1991).
[29]J. P. Perdew, K. Burke, and M. Ernzerhof, "Generalized Gradient Approximation Made Simple," *Phys. Rev. Lett.*, **77**, 3865–8 (1996).
[30]M. Durandurdu, "*Ab Initio* Simulation of Structural Phase Transformation of 2H SiC at High Pressure," *Phys. Rev. B*, **75**, 235204 (2007).
[31]K. Sarasamak, A. J. Kulkarni, M. Zhou, and S. Limpijumnong, "Stability of Wurtzite, Unbuckled Wurtzite, and Rocksalt Phases of SiC, GaN, InN, ZnO, and CdSe under Loading of Different Triaxialities," *Phys. Rev. B*, **77**, 024104 (2008).
[32]H. J. Monkhorst and J. D. Pack, "Special Points for Brillouin-Zone Integrations," *Phys. Rev. B*, **13**, 5188–92 (1976).
[33]R. Hundt, J.C Schön, A. Hannemann, and M. Jansen, "Determination of Symmetries and Idealized Cell Parameters for Simulated Structures," *J. Appl. Crystallogr.*, **32**, 413–6 (1999). □